Journal of
Composites Science

MDPI

Article

Flax–Reinforced Vitrimer Epoxy Composites Produced via RTM

Patricio Martinez * and Steven Nutt

M.C. Gill Composite Center, University of Southern California, Los Angeles, CA 90089, USA
* Correspondence: mart136@usc.edu

Abstract: Composite laminates were produced by RTM using similar glass and flax fabrics and both vitrimer epoxy and aerospace-grade epoxy, both formulated for liquid molding. Tensile and flexural properties were measured and compared, revealing that the vitrimer composites exhibited equivalent performance in flexural strength and tensile modulus, but slightly lower performance in tensile strength relative to reference epoxy composites. In general, glass–fiber composites outperformed flax–fiber composites in tension. However, both glass and flax–fiber composites yielded roughly equivalent flexural strength and tensile modulus-to-weight ratios. Flax fabrics were recovered from composites by matrix dissolution, and a second-life laminate showed full retention of the mechanical properties relative to those produced from fresh flax. Finally, a demonstration of re-forming was undertaken, showing that simple press-forming can be used to modify the composite shape. However, re-forming to a flat configuration resulted in local fiber damage and a decrease in mechanical properties. An alternative forming method was demonstrated that resulted in less fiber damage, indicating that further refinements might lead to a viable forming and re-forming process.

Keywords: resin transfer molding; flax–fibers; glass–fibers; vitrimers; recycled flax–fibers

Citation: Martinez, P.; Nutt, S. Flax–Reinforced Vitrimer Epoxy Composites Produced via RTM. *J. Compos. Sci.* **2024**, *8*, 275. https://doi.org/10.3390/jcs8070275

Academic Editor: Francesco Tornabene

Received: 1 June 2024
Revised: 4 July 2024
Accepted: 11 July 2024
Published: 16 July 2024

1. Introduction

Composite materials are instrumental in efforts to increase the sustainability of systems, enabling increased fuel efficiency, extended vehicle range, and renewable energy structures (wind blades). However, composite materials themselves rank poorly with respect to sustainability, possessing large carbon footprints for production, large production scrap, and no complete recycling pathway at end of life. In this study, we demonstrate the feasibility of producing natural fiber composites comprising a fully recyclable vitrimer epoxy matrix using standard resin transfer molding (RTM). The aim is to demonstrate feasibility and to highlight the merits and drawbacks of the materials and processes, with the expectation that continued efforts to refine and optimize will be demonstrated in the future.

The use of composite materials spans the aerospace, wind energy, marine, automotive, and sports industries. However, production scrap rates are upwards of 30% for carbon fiber composites [1], and there is no viable recycling pathway for matrix materials. The wind-turbine industry alone will generate nearly half a million tons of carbon fiber-reinforced polymer (CFRP) waste by 2050 [2]. Therefore, there is a strong incentive to find recycling methods to reduce such waste. Currently, two of the main methods used for recycling are mechanical and thermal recycling [3]. These methods have downsides: mechanical recycling is achieved by shredding the material, reducing the length and alignment of recovered fibers, and can damage fibers as well [4], serving more as downcycling. Thermal recycling involves pyrolyzing the resin, which can result in close-to-virgin fibers, but requires extreme temperatures, can produce harmful gasses, and eliminates any possibility of recycling the matrix [3]. Chemical recycling can yield close-to-virgin fibers while allowing for reuse of the matrix, although the methods have not been scaled up yet [5,6].

Most carbon fiber recycling focuses on recovering fibers while eliminating and discarding the resin. While carbon fiber constitutes the majority of raw material costs, aerospace-

quality resin prices are not insignificant [7], and discarding it entails waste. In glass–fiber-reinforced polymers (GFRPs), the fibers are much cheaper than carbon [8], and as such, the cost fraction associated with the matrix is significantly larger. Thus, alternative polymers that can be recycled, such as vitrimers, are appealing.

Vitrimers contain thermally reversible covalent bonds that impart processing characteristics normally associated with thermoplastics [9]. Even after curing, vitrimers can be reshaped at elevated temperatures [10]. Furthermore, through a closed-loop process, the vitrimer polymer matrix can be dissolved and reused, leaving the fabric intact [11]. Such a material may be suited to applications in the automotive and sports industries, where minor repairs are more expected than in the aerospace industry and component lifecycles are shorter.

Carbon fiber production is energy-intensive [12], which drives the need to reuse the fibers [13]. Carbon fibers are produced from PAN or pitch precursor fibers, both of which are derived from fossil fuels [14]. One alternative to synthetic fibers is natural fibers derived from plants, which are, thus, renewable. Mechanical properties of natural fibers can approach those of lower-end glass fibers [15]. For applications where the remarkable, exceptional performance of carbon fibers is unnecessary, but weight savings are still important (e.g., automotive), natural fibers may find utility. For this study, flax fibers were selected. Flax fibers have been used in textiles dating back to 5000 BC [16]. Flax fabric has mechanical properties that approach those of glass fibers, but have a much lower density and cost.

Table 1 shows a comparison of select properties of flax, E-glass, and carbon fibers. Flax fibers and fabrics, in principle, offer lower cost and greater sustainability relative to carbon and glass fibers.

Table 1. Comparison of the general properties and cost of flax, glass [17], and carbon fibers [18].

Fiber	Diameter [μm]	Density [10^3 kg/m^3]	Tensile Strength [MPa]	Elastic Modulus [GPa]	Cost [USD/kg]
Flax	12–600	1.4–1.5	343–2000	27.6–103	0.30–1.55
E-Glass	<17	2.5–2.59	2000–3500	70–76	1.65–3.25
Carbon	5–10	1.75–2.18	2000–7000	200–900	>10

Most FRP manufacturing methods, such as autoclave cure, vacuum-bag-only prepreg (VBO), and vacuum infusion (VI), are considered too slow for automotive processes, while high-pressure RTM has been widely practiced. In the present work, resin transfer molding (RTM) was selected to accomplish the project goals. RTM relies on pressurized infusion of low-viscosity resin into a rigid closed mold containing a dry fabric preform [19]. Once fully infused, the mold is heated, and the part is cured and subsequently demolded. By increasing the injection pressure, it is possible to reduce the cycle time to under 10 min [20], and the process produces a net-shape part requiring little finishing.

The objective of this study is to demonstrate the feasibility of producing recyclable flax–vitrimer composites via RTM. The tests matrix consisted of two reinforcements: flax and glass fabrics and two matrices—vitrimer epoxy and a commercial epoxy. The mechanical properties of the product composites highlight the relative merits and limitations of the less common constituents—flax and vitrimer epoxy—relative to conventional fibers and matrices. A complete recycling pathway of the vitrimer composite is demonstrated and evaluated, along with its capacity for forming and re-forming. The study demonstrates the use of lab-scale methods to evaluate how new materials perform in manufacturing processes, an effort that helps to identify potential challenges for scale-up and insertion into practice.

2. Materials and Methods

2.1. Resins

Two resins were selected: a vitrimer epoxy (Vitrimax T130, Mallinda Inc., Denver, CO, USA), and an epoxy resin (RTM-6, Hexcel, Stamford, CT, USA), which was used as a baseline for comparison.

The commercial epoxy was cured following the manufacturer's recommended cure profile. For the vitrimer epoxy resin, isothermal rheology tests were performed to determine a suitable infusion temperature, maximizing the time during which the viscosity was less than 1 Pa·s, −55 °C. The rheology plots for standard infusion-and-cure cycles for both resins are shown in Figure 1. Unlike the vitrimer epoxy, the viscosity of the commercial epoxy resin remained low (below 1 Pa·s) for the entire infusion cycle. In contrast, the vitrimer resin sustained low viscosity (<1 Pa·s) for ~20 min, with the viscosity steadily increasing from the moment of mixing. This behavior effectively limited the resin pot-life and required infusion immediately after mixing. Vitrimer gelation occurred during the temperature ramp to the first dwell for the vitrimer, while the commercial epoxy gelled approximately 20 min into the 2 h dwell (cure).

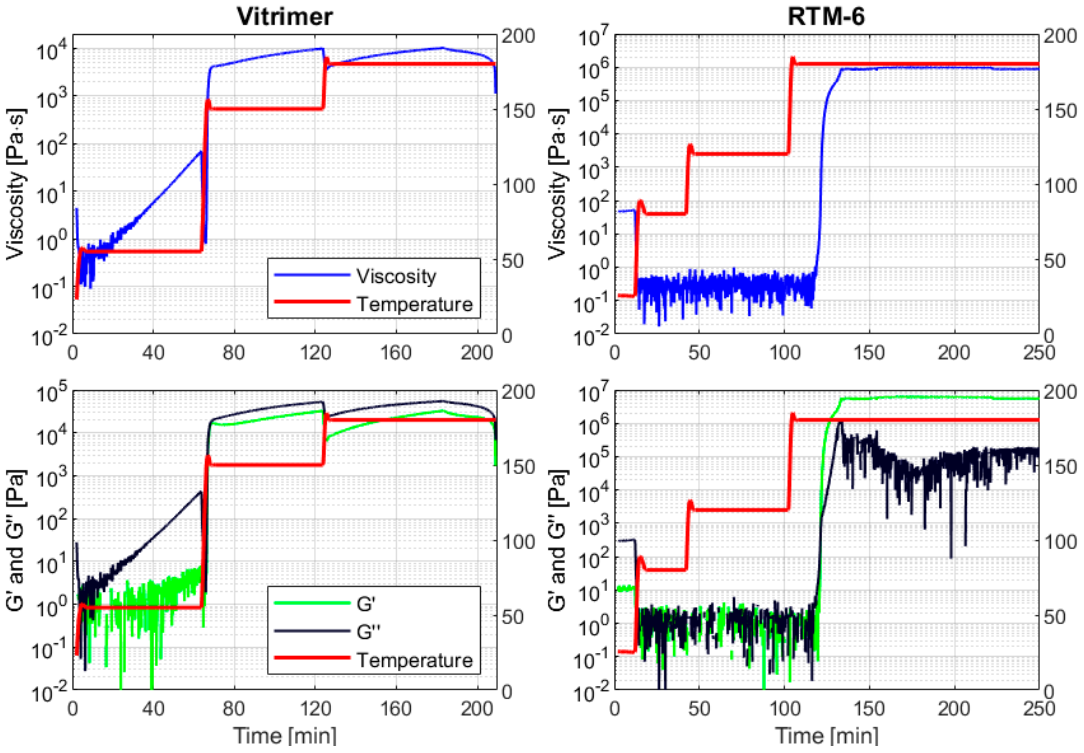

Figure 1. Rheology graphs for Vitrimax T130 (**left**) and RTM-6 (**right**) following the specific injection-and-cure temperature cycles used for each resin.

2.2. Fabrics

The three fabrics used included a 2 × 2 twill flax fabric with areal weight 200 g/m^2, a 2 × 2 twill glass fabric with similar areal weight (GF-22-200-100, Easy Composites, Ltd., Stoke-on-Trent, UK), and a recycled flax fabric recovered from a flax–vitrimer composite. The recycled fabric was extracted by first placing the flax–vitrimer laminate in a solution of resin precursors. Due to the specific chemistry of the vitrimer, the matrix underwent a bond exchange within the solution, resulting in depolymerization. After 24 h, the fabric was removed, rinsed with ethanol, and dried [11]. Surface micrographs of the three fabrics are shown in Figure 2 (VHX-5000, Keyence, Itaska, IL, USA). Note the smaller tow-size of the glass fabric relative to the flax. The only apparent distinction between virgin and recycled flax is a slight discoloration of the recycled fabric.

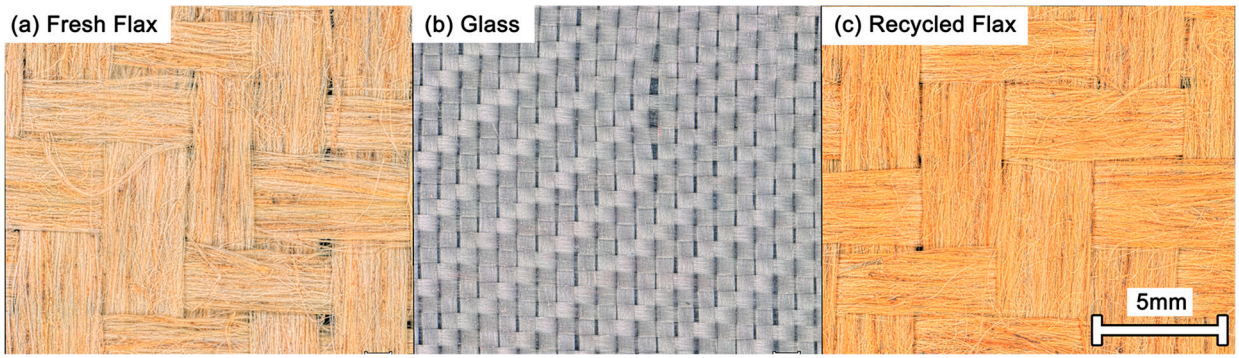

Figure 2. Surface micrographs of the virgin flax (**a**), glass (**b**), and recycled flax (**c**) fabrics.

The general characteristics of the three fabrics are tabulated in Table 2. Areal weight was measured by weighing individual plies of each fabric, while density was measured using a gas pycnometer (Micromeritics, Accupyc 1330, Norcross, GA, USA) and thickness was measured with digital calipers. Tow width was measured from the micrographs in Figure 2. The three fabrics had similar areal weights, but the uncompressed thickness of the glass fabric was ~1/3 of the flax fabric. Similarly, the density of the glass fabric was roughly 50% greater than the flax. The tow widths were also narrower in the glass fabric, allowing for a tighter weave and a more flexible fabric. There was a negligible difference in the physical properties of the virgin and recycled flax fabrics.

Table 2. General properties for fabrics used in this study.

Fabric	Weave	Areal Weight [g/m^2]	Density [10^3 kg/m^3]	Uncompressed Thickness [mm]	Tow Width [mm]
Flax	2 × 2 Twill	202 ± 6	1.46 ± 0.03	0.43 ± 0.02	2.58 ± 0.37
Glass	2 × 2 Twill	200 ± 7	2.57 ± 0.01	0.14 ± 0.01	0.71 ± 0.04
Recycled Flax	2 × 2 Twill	207 ± 7	1.47 ± 0.01	0.43 ± 0.02	2.69 ± 0.32

Preforms for RTM were produced from 160 × 90 mm plies—12 for the flax fabrics and 23 for the glass fabrics, to achieve comparable thickness. A thin layer of binder (Airtac Mega, Airtech, Huntington Beach, CA, USA) was sprayed onto the top surface of the first ply, and a second ply was aligned on top. Using a custom mold, the stack was then compressed under ~500 kPa for 5 min at room temperature using a hot press (Genesis, Wabash MPI, Wabash, IN, USA). After pressing, the preform was weighed and measured before repeating the process for the next ply until a preform thickness of approximately 3.1 mm was achieved. Once fully consolidated, preforms were trimmed to 150 × 80 mm (3 × 5 in).

2.3. RTM Part Production

A custom-built test cell (dubbed 'mini-RTM') was used to produce composite plates, as shown in Figure 3. The test cell allowed for temperature and pressure measurements within the mold while featuring a glass window for direct observation during infusion [21].

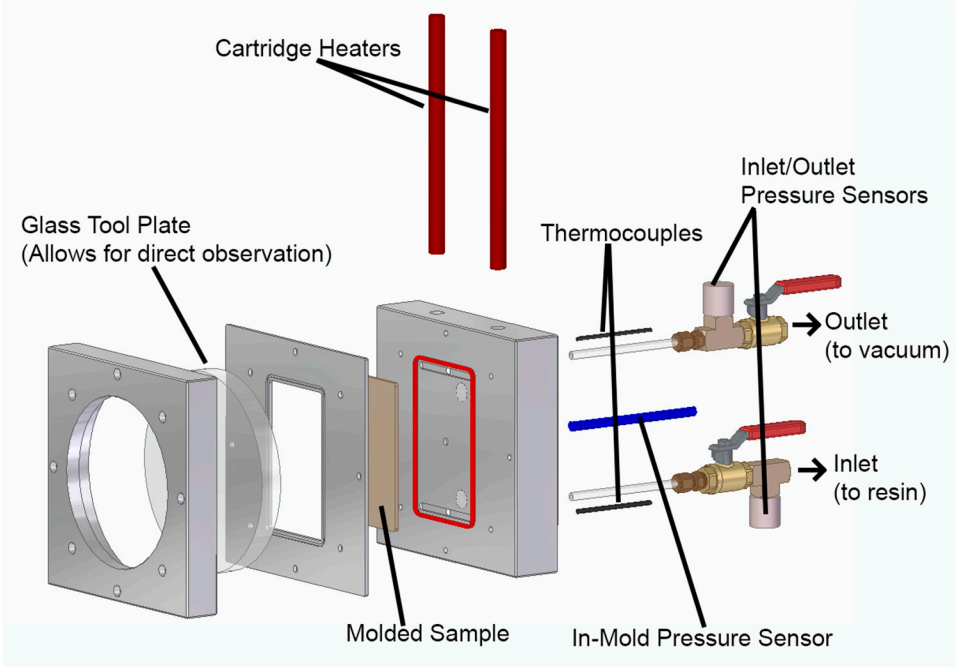

Figure 3. Test cell used to produce laminates in this study [21].

Leak testing was undertaken to ensure a satisfactory seal, and resin was infused following procedures specific to the resin used. The vitrimer resin was mixed, then immediately vacuum-degassed for 5 min. Resin was poured into a pressure pot and heated to 55 °C. The mold was also heated to 55 °C. The pressure pot was pressurized to 350 kPa (50 psi), and resin was allowed to infuse. After saturation, the outlet was sealed and the mold was heated to 150 °C. The laminate was cured at 150 °C for 60 min, then post-cured at 180 °C for 60 min. The procedure for the commercial epoxy was similar, although the pressure pot was held at 70 °C and the mold at 120 °C during infusion. Finally, the cure lasted 2 h at 180 °C. The cure cycles are shown in the rheology curves of Figure 1. After curing, select cross-sections were examined to investigate the microstructural features of the different laminates. Two sets of cross-sections were produced: a full set of abrasive polished sections for general inspection and a flax and glass cross-section produced using an ion polisher (JEOL IB-09010CP, Peabody, MA, USA) for higher resolution microscopy. The test matrix of the parts produced in this study is shown in Table 3.

Table 3. Test matrix detailing the specifics of all parts produced for this study.

Sample	Fabric	Resin	Num Plies
FV-1	Flax	Vitrimer	13
FV-2	Flax	Vitrimer	12
FR	Flax	RTM6	12
GV	Glass	Vitrimer	23
rFV	Recycled Flax	Vitrimer	12

Following demolding, all laminates were characterized. Thickness and density were measured, and the volume fraction was calculated based on the density of the laminate (ρ_c), the matrix (ρ_m), and the fabric (ρ_f) through the rule of mixtures given in Equation (1).

$$V_f = \frac{\rho_c - \rho_m}{\rho_f - \rho_m} \quad (1)$$

2.4. Re-Forming

A tool was designed for reshaping flax–vitrimer composites (Figure 4). The matched metal tool featured a 20° and 25.4 mm radius convex and concave corner. Threaded holes were included in the lower tool, with matching unthreaded holes in the upper tool, to allow for positioning of threaded rods for alignment.

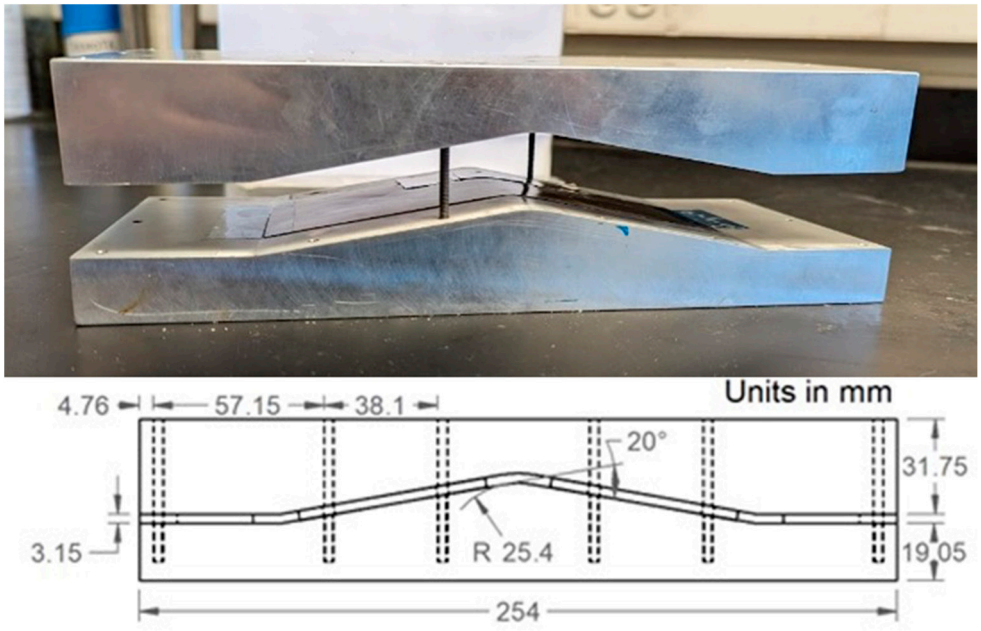

Figure 4. Tool used for bending of vitrimer parts. (**Top**) A picture of the tool. (**Bottom**) Schematic.

The forming trials were conducted with Sample FV-2. The laminate was cut into five coupons, the first three of which were 19 × 127 mm, and these were used for mechanical tests, while the remaining two were 19 × 63.5 mm and were used to prepare polished sections. Two of the three full-sized coupons and both half-length coupons were subjected to bending, and all half-length coupons but one were subsequently straightened. Coupons were prepared by cutting the cured laminate using a waterjet cutter (ProtoMAX, Omax Corporation, Kent, WA, USA). After cutting, coupons were allowed to air-dry for at least 24 h.

The bending process began by pre-heating both sides of the tool to 140 °C. The composite coupon was then carefully positioned over the center of the corner, and the top tool was replaced. The entire tool was then re-heated for 15 min before cooling on an aluminum plate for 45 min and demolding. Straightening followed the same procedure, replacing the matched tool with two aluminum plates while using the top tool as a weight on top of the upper plate. In both cases, no external pressure was applied, and the compaction force on the laminate was derived from the weight of the top tool (1.9 kg).

2.5. Mechanical Testing

Two types of mechanical tests were conducted. Tensile tests in accordance with ASTM D3039 [22] provided the tensile strength and Young's modulus, both fabric-dominated properties. Short-beam-shear tests (ASTM D638 [23]) provided the flexural strength, a matrix-dominated property. All tests were performed on a load frame (Universal Testing Machine 5567, Instron, Norwood, IL, USA), and displacements were measured using a 3D DIC system (ARAMIS, Trilion, King of Prussia, PA, USA).

3. Results and Discussion

3.1. Cured Laminate General Properties

The general properties of the laminates are shown in Table 4. The initial flax–vitrimer panel (FV-1) was produced using 13 plies, although subsequent plates were produced with 12 plies. Note that the plates produced with flax had higher volume fraction and lower thickness than the plate produced with glass. Also, all flax laminates had densities roughly 75% of the densities of the glass composite plates (despite a higher fiber volume fraction) due to the lower density of flax fabric.

Table 4. General properties of the cured laminates.

ID	Num of Plies	Thickness [mm]	V_f [%]	Density [10^3 kg/m^3]
FV-1	13	3.35 ± 0.05	59 ± 4	1.302 ± 0.003
FV-2	12	3.24 ± 0.02	54 ± 4	1.280 ± 0.005
GV	23	3.58 ± 0.04	45 ± 1	1.751 ± 0.015
FR	12	3.18 ± 0.04	48 ± 4	1.291 ± 0.001
rFV	12	3.19 ± 0.04	53 ± 2	1.284 ± 0.001

Cross-sections are shown in Figure 5. The distinct color difference for the FR part (Figure 5b), which allows for observation of the 0° fibers, is attributed to the different matrix formulation. The significant void content in the glass laminate (GV) (Figure 5c) is attributed to the tighter weave leading to greater air entrapment: The vitrimer resin exhibited off-gassing during infusion, entrapping gas. Resin-rich pockets were observed in the glass laminate, although further from the inlet and outlet side (the top of the cross-section), these same pockets contained large voids. Finally, both FV-1 and rFV plates showed negligible differences (Figure 5a,d), showing that virgin and recycled flax fabrics yielded similar microstructures.

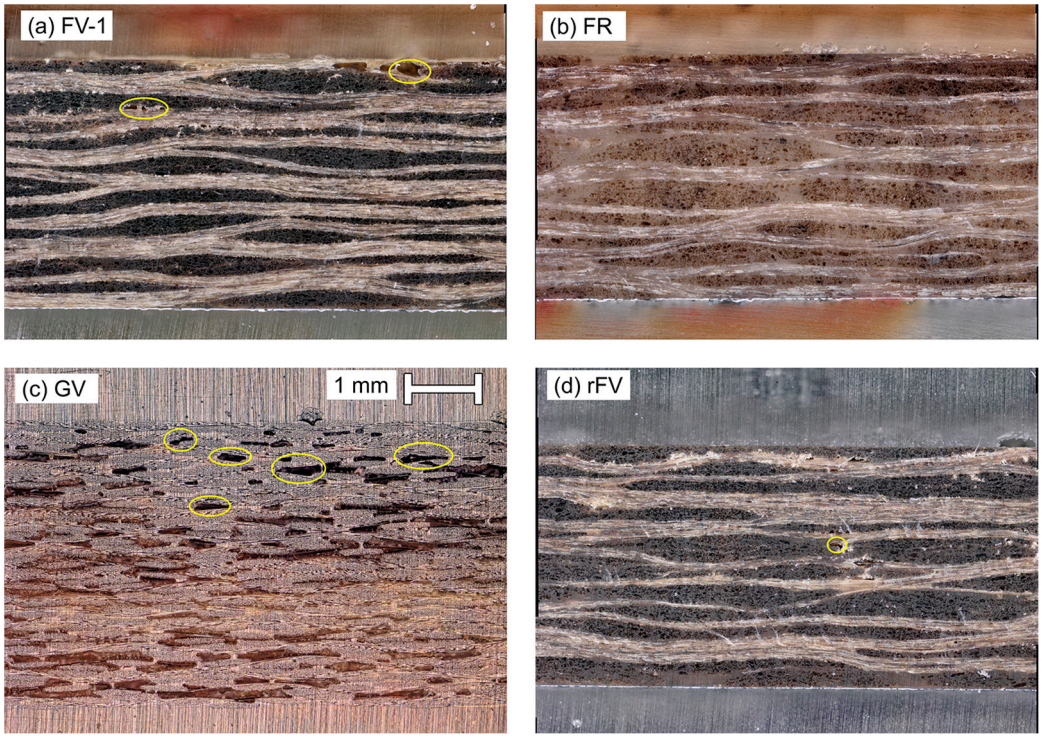

Figure 5. Cross-section micrographs for select laminates. (**a**) FV-1, (**b**) FE, (**c**) GV, (**d**) rFV. Some visible voids are circled in yellow.

The ion-polished cross-sections of FV-1 and GV, allowing for observation of the individual fiber bundles, are shown in Figure 6, highlighting important differences between the

two fibers. First, glass fibers were uniformly round, with an average diameter of 12 ± 2 µm, while flax fibers varied widely and were irregular, roughly rectangular or elliptical. Flax fibers showed a width-to-height ratio of 1.7 ± 0.5, the shorter dimension being 15 ± 4 µm and the larger being 25 ± 5 µm. Furthermore, the flax fibers were often aggregated, with the edges of individual fibers conforming to the shape of neighboring fibers. Some aggregates were so tight that the edges of individual fibers could not be easily discerned. Finally, the lumen in each fiber appeared as a thin channel at the fiber center; often resembling a void, but sometimes filled with matrix.

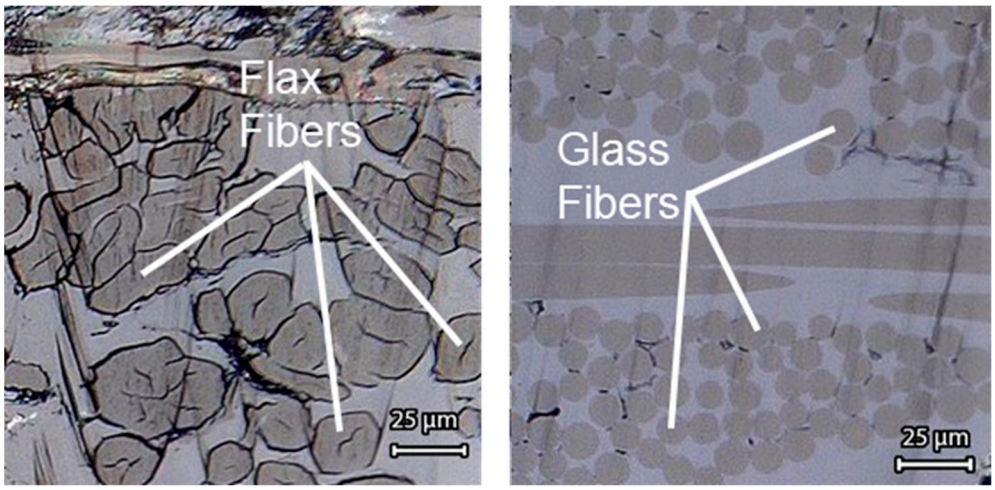

Figure 6. High-resolution cross-sections of (**left**) sample FV-1 and (**right**) sample GV.

3.2. Mechanical Properties

Figure 7 shows the results of select tensile tests for each laminate. Note that the GV plate surpassed the other laminates in tensile strength and modulus, showing a distinct performance gap between the two types of fibers. All three flax laminates were grouped close together, with the stress–strain curves nearly overlapping.

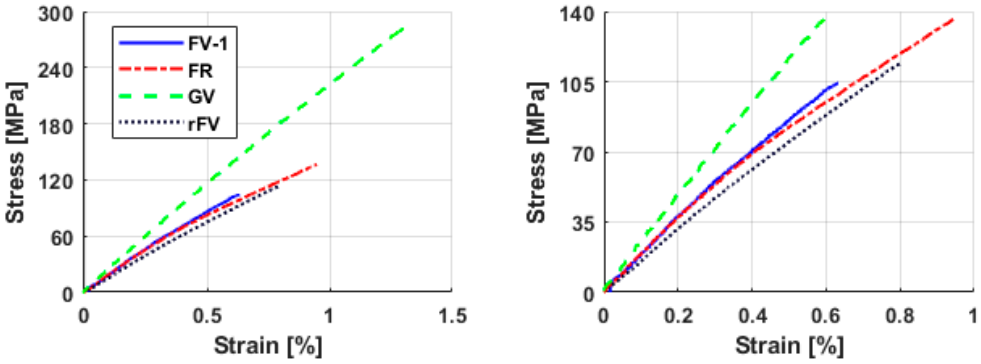

Figure 7. Tensile test results for all currently produced samples. (**left**) Entire curves displayed. (**right**) Close-up of the flax laminates.

The mechanical properties of all laminates are summarized in Figure 8a, highlighting the differences in the tensile properties of flax and glass laminates. Comparing FV-1 and GV, the glass composite tensile strength was nearly 200% greater than the flax laminate, while the modulus was ~33% greater, despite the significant void content in the glass laminate. Comparing the different matrix materials, the tensile strength of FR was 27 ± 9% greater than FV-1, while the tensile modulus for the FR plate was 15 ± 4% less than that of FV-1. Comparing the flexural strength obtained via short-beam shear tests, the flex strength of

FR was 30 ± 18% greater than FV-1, while the strength of GV was within the same bounds, with the flex strength being 7 ± 11% greater than FV-1.

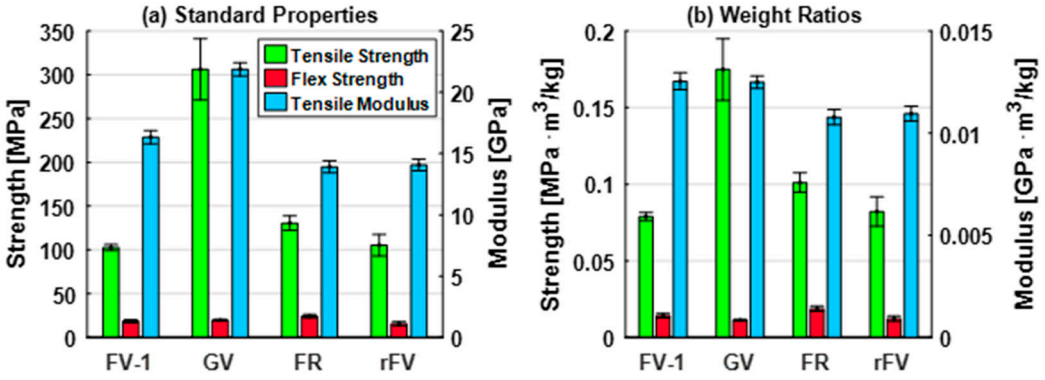

Figure 8. Mechanical properties for all coupons. (**a**) Standard bar graph. (**b**) Properties divided by density.

Despite having undergone the recycling process, the part with recycled fabric exhibited mechanical properties similar to the fresh flax part. The laminate produced with recycled flax fabric (rFV) showed tensile and flex strength approximately equivalent to the fresh flax fabric laminate (FV-1), within 3 ± 12% and 16 ± 15%, with only a slight decrease in the elastic modulus (14 ± 4%).

The strength-to-weight and modulus-to-weight ratios of the laminates are shown in Figure 8b. The glass–fiber plate exhibited a greater tensile strength-to-weight ratio (122 ± 26%) than the flax composite. However, the modulus-to-weight ratio was approximately equal (within 4%), presumably because the greater weight of the glass fabric compensated for the difference in the modulus. Furthermore, the flexural strength-to-weight ratio was lower for GV (21 ± 8% less) than for FV-1, which was not unexpected. Flexural strength tends to be matrix-dominated, and increased fiber stiffness typically causes only a modest increase in flexural strength. This phenomenon was offset by the lower fiber volume fraction and increased void content in the glass laminate. Thus, the two types of laminates yielded similar strengths, and thus, the GF laminate yielded a notably lower strength-to-weight ratio.

3.3. Re-Forming

Laminate FV-2 was cut into five coupons (Table 5). Changes to the coupon thickness were recorded during the initial forming (bending) and following re-forming (straightening), as shown in Figure 9. After initial forming, the average thickness increased by 4.1 ± 0.5% across coupons 2–5. Following re-forming to flat coupons, the thickness decreased on average by 0.8 ± 0.5%, and a total average thickness increase of 3.9 ± 0.3% occurred after the two-step forming process.

Table 5. Coupons cut from FV-2 and used for the reshaping trials.

Coupon #	Processing	Testing
1	None	Tensile
2	Bending and Straightening	Tensile
3	Bending and Straightening	Tensile
4	Bending	Micrograph
5	Bending and Straightening	Micrograph

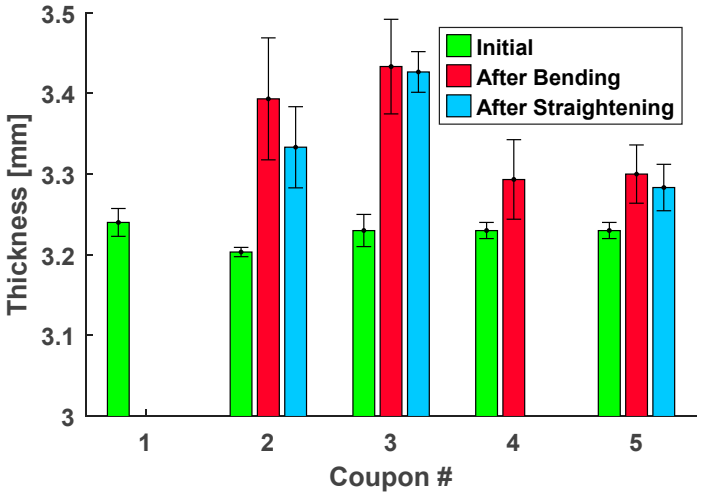

Figure 9. Thickness values of the coupons cut from FV-2 after different degrees of reshaping.

Bend-forming consistently caused a distinct defect, visible as a protrusion on the coupon facing the convex tool. A similar defect was observed on the opposite side of the coupons after re-forming. The protrusion appeared on the side of the coupon experiencing compression each time, likely due to the fiber buckling under compression.

Polished sections of the corner region at different junctures during forming/re-forming are shown in Figure 10. The surface defect was associated with fiber buckling, as shown in Figure 10a, albeit to a lesser degree. Wrinkles in the fabric were confined to the upper half of the plate, corresponding to regions under compression. After re-forming (flattening), fiber waviness was reduced, but not eliminated (Figure 10b).

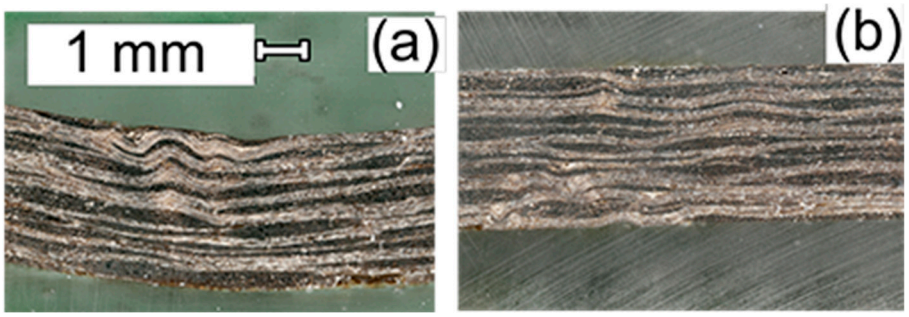

Figure 10. Micrographs of the center region of reshaped coupons. (**a**) Coupon 4 after initial bending. (**b**) Coupon 5 after subsequent straightening.

Tensile testing was performed on the first three coupons after re-forming (Figure 11). Coupons 2 and 3 failed along the trace of the former corner bend. All three coupons followed a similar initial linear curve before deflecting to a less steep secondary curve for the re-formed coupons 2 and 3. While the modulus was negligibly greater for the re-formed coupons ($5 \pm 2\%$), the tensile strength decreased (by nearly 50%). Re-forming caused negligible changes to the elastic properties, but weakened the fibers such that they failed at half the stress.

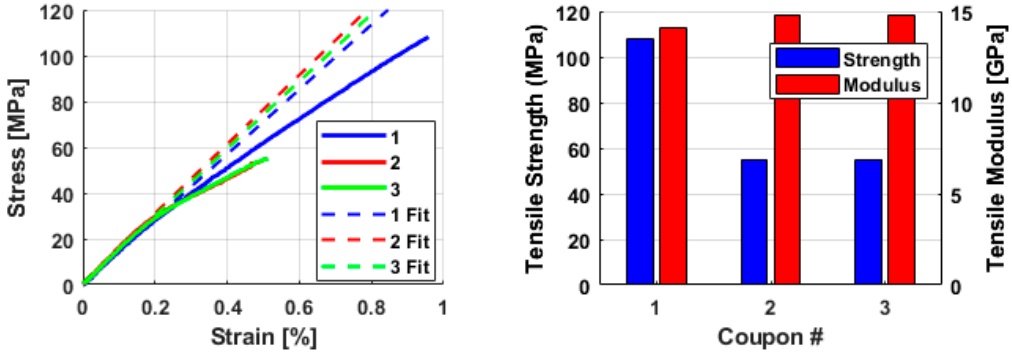

Figure 11. Results of the tensile testing of sample FV-2, with coupon 1 being as is and coupons 2 and 3 having undergone bending and straightening. (**Left**) Stress vs. strain curve for each coupon, with the fitted curve used to determine the tensile modulus. (**Right**) Bar graph showing the aggregate tensile properties for each coupon.

Further insight into the observed strength reduction was provided by sections of the tested coupons (Figure 12). At sites remote from the bend, the buckling of the fabric fibers was negligible. Comparing Coupon 1 to Coupons 2 and 3 at the edges of the cross-section revealed negligible differences. However, at the point of fracture, the fibers at the mid-plane of the beam showed distinct differences. In Coupon 1, the fibers remained unbent, while in Coupons 2 and 3, the fibers were bent away from the centerline. The shaping processes damaged and displaced fibers such that they were no longer aligned with the loading direction. Fiber misalignment led to premature failure and decreased tensile strength.

Figure 12. Micrographs of select FV-2 coupons after tensile testing.

Using a hand-roller, an attempt was made to reduce the fabric distortion from bend-forming. Gradual bending should allow fibers to conform to the corner more easily and prevent or minimize the observed buckling and wrinkling. This process followed a similar procedure to the forming process: the tool was heated to 140 °C, the coupon was aligned with the corner of the tool, and the roller was used to force the coupon to bend. Once the coupon was fully bent, the top tool was positioned, and the process was resumed as before. The coupons were not long enough for tensile testing after re-forming. However, a similar-sized coupon was bent using the standard method, and the cross-sections of both were compared (Figure 13). The laminate formed using the roller showed no defects, while

the laminate formed without roller application showed distinct wrinkling on the concave side (yellow ellipses, Figure 13a).

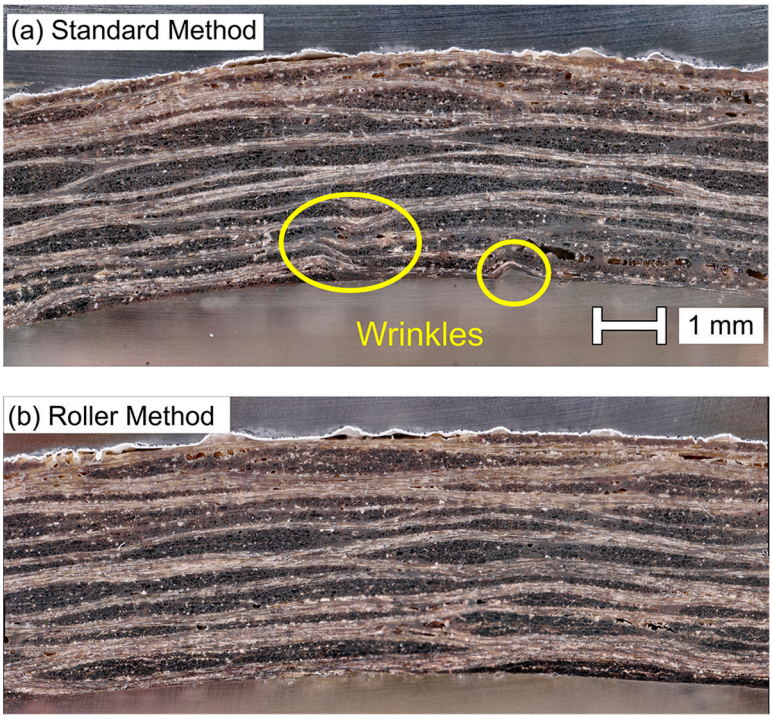

Figure 13. Cross-sections of bent coupons. (**a**) Standard pressing method with major defects highlighted; (**b**) hand roller method.

4. Conclusions

Woven flax fibers were well-suited to RTM and yielded porosity-free composite plates, while glass–fiber composites showed porosity because of the finer weave fabric. Flax fabric composites also yielded superior flex strength-to-weight ratios and comparable tensile modulus-to-weight ratios relative to the glass–fiber composites. Despite these advantages, glass–fiber composites exhibited superior tensile strength values (~200% greater), which was not unexpected in light of the reference values. However, because composite applications are often compression-critical and subject to multi-axial loads, there may be potential to substitute flax fabrics for glass fabrics in specific instances. One drawback to the future use of flax–fiber composites stems from the observed variability in fiber size and dispersion within a given batch of fabric. Compounding this issue are reports of batch-to-batch variability that will manifest in variations in mechanical properties. Such variability, along with the shortage of property data and experience, must be addressed before the use of flax fibers can be widespread.

Natural fibers such as flax are a "greener" alternative to synthetic fibers, and as such, they may be useful substitutes for synthetic fibers, particularly in applications where increased sustainability is sought and lower performance levels can be tolerated. These opportunities may emerge in large-volume applications (wind blades, electric vehicles) because of the potential to significantly reduce carbon footprint. However, even with natural fiber reinforcements, composites will still be sent to landfills at the end of their life, highlighting the need for solutions to composite recycling. Recycling solutions, if developed, may well change the calculus of fiber sustainability.

The vitrimer epoxy used here offers the prospects of increased sustainability as well as exceptional formability. As was shown, the strength of the vitrimer laminates was approximately 30% less than the laminates produced with commercial epoxy in both tension and flex, but the tensile modulus was matched. Furthermore, recovered flax fibers were virtually indistinguishable from fresh flax fibers and yielded composites with

nearly identical mechanical performances. However, the processing characteristics of the commercial epoxy (pot life, fusion time, minimum viscosity, ease of cleanup) were superior to those of the vitrimer epoxy. Nevertheless, this difference is expected to narrow with future refinements.

Natural fibers undoubtedly afford one avenue towards increased sustainability, and the use of vitrimer epoxy matrices complements that approach. First and foremost, the vitrimer epoxy matrix allows for convenient separation of fabric and cured matrix at room temperature, affording the possibility of repeated re-use, as opposed to downcycling at end of life via pyrolysis. Furthermore, vitrimers greatly expand the processing space of thermoset composites, allowing for joining by welding, thermo-forming, and repairs. These attributes are expected to compensate for the aforementioned drawbacks to natural fibers and to offer a viable pathway for insertion into practice.

Author Contributions: P.M.: conceptualization, methodology, validation, investigation writing—original draft preparation. S.N.: conceptualization, resources, writing—review and editing, supervision, funding acquisition. All authors have read and agreed to the published version of the manuscript.

Funding: This research was funded by Mallinda, Inc., through the Department of Energy, SBIR grant number #SC0022864.

Data Availability Statement: The authors confirm that the data supporting the findings of this study are available within the article.

Acknowledgments: The authors would like to acknowledge the following people: Philip Tayton and Jack Burns at Mallinda Inc. for support and technical assistance with the vitrimer resin; Mark Anders for support with and initial development of the "mini-RTM" test cell; and undergraduate research assistants Ryan Kraemer and Andrius Stankus for experimental assistance.

Conflicts of Interest: Authors Patricio Martinez and Steven Nutt received research funding from Mallinda, Inc. Mallinda, Inc. supplied the vitrimer epoxy resin and the recycled flax fabric used in the study, but the company had no role in the design of the study, the collection, analysis or interpretation of the data, in the writing of the manuscript or in the decision to publish the results.

References

1. Khurshid, M.F.; Hengstermann, M.; Hasan, M.M.B.; Abdkader, A.; Cherif, C. Recent developments in the processing of waste carbon fibre for thermoplastic composites—A review. *J. Compos. Mater.* **2020**, *54*, 1925–1944. [CrossRef]
2. Lefeuvre, A.; Garnier, S.; Jacquemin, L.; Pillain, B.; Sonnemann, G. Anticipating in-use stocks of carbon fibre reinforced polymers and related waste generated by the wind power sector until 2050. *Resour. Conserv. Recycl.* **2019**, *141*, 30–39. [CrossRef]
3. Isa, A.; Nosbi, N.; Ismail, M.C.; Akil, H.M.; Ali, W.F.F.W.; Omar, M.F. A Review on Recycling of Carbon Fibres: Methods to Reinforce and Expected Fibre Composite Degradations. *Materials* **2022**, *15*, 4991. [CrossRef] [PubMed]
4. Yang, Y.; Boom, R.; Irion, B.; van Heerden, D.J.; Kuiper, P.; de Wit, H. Recycling of composite materials. *Chem. Eng. Process. Process Intensif.* **2012**, *51*, 53–68. [CrossRef]
5. Yu, Z.; Lim, Y.J.; Williams, T.; Nutt, S. A rapid electrochemical method to recycle carbon fiber composites using methyl radicals. *Green Chem.* **2023**, *25*, 7058–7061. [CrossRef] [PubMed]
6. Navarro, C.A.; Giffin, C.R.; Zhang, B.; Yu, Z.; Nutt, S.R.; Williams, T.J. A structural chemistry look at composites recycling. *Mater. Horiz.* **2020**, *7*, 2479–2486. [CrossRef]
7. Meng, F.; McKechnie, J.; Pickering, S.J. An assessment of financial viability of recycled carbon fibre in automotive applications. *Compos. Part A Appl. Sci. Manuf.* **2018**, *109*, 207–220. [CrossRef]
8. Bader, M.G. Selection of composite materials and manufacturing routes for cost-effective performance. *Compos. Part A Appl. Sci. Manuf.* **2022**, *33*, 913–934. [CrossRef]
9. Post, W.; Susa, A.; Blaauw, R.; Molenveld, K.; Knoop, R.J.I. A Review on the Potential and Limitations of Recyclable Thermosets for Structural Applications. *Polym. Rev.* **2020**, *60*, 359–388. [CrossRef]
10. Taynton, P.; Yu, K.; Shoemaker, R.K.; Jin, Y.; Qi, H.J.; Zhang, W. Heat- or water-driven malleability in a highly recyclable covalent network polymer. *Adv. Mater.* **2014**, *26*, 3938–3942. [CrossRef]
11. Taynton, P.; Ni, H.; Zhu, C.; Yu, K.; Loob, S.; Jin, Y.; Qi, H.J.; Zhang, W. Repairable woven carbon fiber composites with full recyclability enabled by malleable polyimine networks. *Adv. Mater.* **2016**, *28*, 2904–2909. [CrossRef] [PubMed]
12. Asmatulu, E.; Overcash, M.; Twomey, J. Recycling of Aircraft: State of the Art in 2011. *J. Ind. Eng.* **2013**, *2013*, 960581. [CrossRef]
13. Meng, F.; McKechnie, J.; Turner, T.; Wong, K.H.; Pickering, S.J. Environmental Aspects of Use of Recycled Carbon Fiber Composites in Automotive Applications. *Environ. Sci. Technol.* **2017**, *51*, 12727–12736. [CrossRef] [PubMed]

14. McLaren, J. *The Technology Roadmap for Plant/Crop-Based Renewable Resources 2020*; National Renewable Energy Lab: Golden, CO, USA, 1999. Available online: https://www.osti.gov/biblio/756319 (accessed on 17 July 2023).
15. Saheb, D.N.; Jog, J.P. Natural fiber polymer composites: A review. *Adv. Polym. Technol.* **1999**, *18*, 351–363. [CrossRef]
16. Yan, L.; Chouw, N.; Jayaraman, K. Flax fibre and its composites—A review. *Compos. B Eng.* **2014**, *56*, 296–317. [CrossRef]
17. Dittenber, D.B.; Gangarao, H.V.S. Critical review of recent publications on use of natural composites in infrastructure. *Compos. Part A Appl. Sci. Manuf.* **2012**, *43*, 1419–1429. [CrossRef]
18. Liu, Y.; Kumar, S. Recent progress in fabrication, structure, and properties of carbon fibers. *Polym. Rev.* **2012**, *52*, 234–258. [CrossRef]
19. Rackers, B. *Resin Transfer Moulding for Aerospace Structures*; Springer: Dordrecht, The Netherlands, 1998. [CrossRef]
20. Vita, A.; Castorani, V.; Germani, M.; Marconi, M. Comparative life cycle assessment of low-pressure RTM, compression RTM and high-pressure RTM manufacturing processes to produce CFRP car hoods. *Procedia CIRP* **2019**, *80*, 352–357. [CrossRef]
21. Anders, M.; Lo, J.; Centea, T.; Nutt, S.R. Eliminating volatile-induced surface porosity during resin transfer molding of a benzoxazine/epoxy blend. *Compos. Part A Appl. Sci. Manuf.* **2016**, *84*, 442–454. [CrossRef]
22. *ASTM D3039*; Standard Test Method for Tensile Properties of Polymer Matrix Composite Materials, 2017th ed. ASTM International: West Conshohocken, PA, USA, 2017. [CrossRef]
23. *ASTM D2344*; Standard Test Method for Short-Beam Strength of Polymer Matrix Composite Materials and Their Laminates. ASTM International: West Conshohocken, PA, USA, 2022. [CrossRef]